Operation of Class-E^2 DC-DC Converter Outside Nominal Conditions

Tomoharu Nagashima† , Xiuqin Wei††, and Hiroo Sekiya†

†Graduate School of Advanced Integration Science, Chiba University
1-33, Yayoi-cho, Inage-ku, Chiba, 263-8522 Japan
††Department of Electronics Engineering and Computer Science, Fukuoka University
8-19-1 Nanakuma, Jonan-ku, Fukuoka 814-0180, Japan

Abstract—In this paper, a steady-state analysis of the class-E^2 dc-dc converter outside the class-E zero-voltage switching and zero-derivative switching (ZVS/ZDS) conditions is presented. Steady-state behaviors of the class-E^2 dc-dc converter outside class-E ZVD/ZDS conditions can be investigated by using the analytical expressions derived in this paper. By carrying out the circuit experiments, it is shown that the analytical predictions agree with the experimental results quantitatively, which validates the accuracy of our analytical expressions.

1. Introduction

The class-E^2 dc-dc converter [1], [2] is one of the resonant converters and is expected to be useful for many applications. The class-E^2 dc-dc converter consists of the class-E inverter [3], and class-E rectifier [4]. By satisfying the class-E zero voltage and zero derivative switching (ZVS/ZDS) conditions on both the inverter and rectifier, the class-E^2 dc-dc converter can achieve high efficiencies at high frequencies. The converter operation satisfying the class-E ZVS/ZDS conditions is called as "nominal conditions" in this paper.

In previous studies [1], [2], steady-state analyses of the class-E^2 dc-dc converter was presented. These studies, however, discuss the class-E^2 dc-dc converter under the class-E ZVS/ZVS conditions. In real electrical applications, the circuit parameters, especially load resistance, vary from the nominal values. Therefore, it is important to comprehend the circuit behavior and performance of the class-E^2 dc-dc converter outside nominal conditions. Analytical expressions cultivate designer's fundamental understanding and intuition. By using the analytical expressions, much additional information, such as ZVS region, can be easily obtained.

This paper presents a steady-state analysis of the class-E^2 dc-dc converter outside nominal conditions. Steady-state behaviors of the class-E^2 dc-dc converter outside nominal conditions can be investigated by using the analytical expressions derived in this paper. By carrying out the circuit experiments, it is shown that the analytical predictions agree with the experimental results quantitatively, which validates the accuracy of our analytical expressions.

2. Circuit Description

Figure 1 shows a circuit topology and example waveforms of the class-E^2 dc-dc converter [1], [2]. The class-E^2 dc-dc converter consists of the class-E inverter [3], and the class-E rectifier [4]. Because both the class-E inverter and the class-E rectifier satisfy the class-E ZVS/ZDS conditions, the class-E^2 dc-dc converter can achieve high power conversion efficiencies at high frequencies.

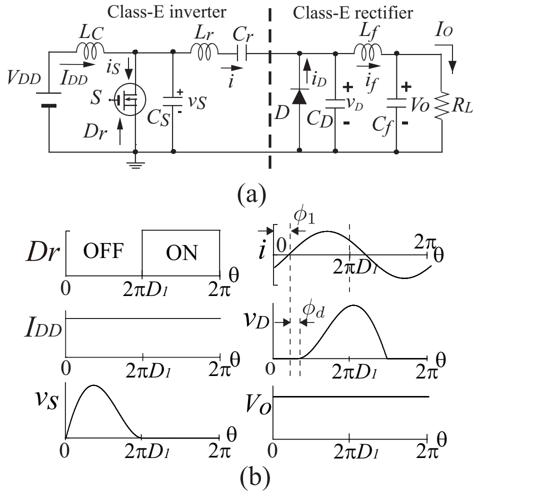

Figure 1: Class-E^2 dc-dc converter. (a) Circuit description. (b) Example waveforms.

2.1. Class-E Inverter

The class-E inverter consists of dc-supply voltage V_{DD}, dc-feed inductance L_C, MOSFET S, which works as a switching device, shunt capacitance C_S , and series resonant network $L_r - C_r$, as shown in Fig. 1(a). The switch of the inverter is driven by the driving signal D_r. During the switch-off interval, the difference of currents through the dc-feed inductor and the resonant filter flows through the shunt capacitor. The current through the shunt capacitor produces the switch voltage. The most important operation of the class-E inverter is that the class-E ZVS/ZDS conditions are satisfied at the turn-on instant as shown in Fig. 1(b). The class-E ZVS/ZDS conditions are expressed as

$$v_S(2\pi D_1) = 0 \quad \text{and} \quad \left.\frac{dv_S}{d\theta}\right|_{\theta=2\pi D_1} = 0, \tag{1}$$

where $\theta = \omega t$ and D_1 are the angular time and the switch-off duty ratio, respectively. Because of the class-E ZVS/ZDS conditions, the class-E inverter achieves high power conversion efficiencies under high frequency operations. Because the class-E inverter usually has a resonant filter with high quality factor, the current through the resonant filter i is regarded as a sinusoidal waveform, which is the input signal of the rectifier.

Figure 2 shows the switching patterns of the class-E

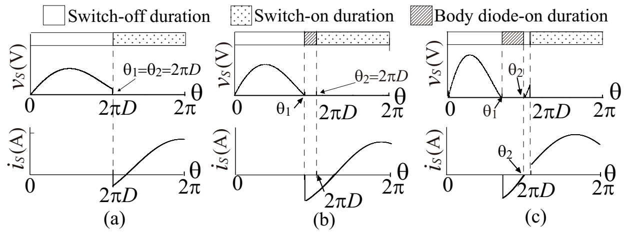

Figure 2: Switching patters of class-E inverter. (a) Case 1. (b) Case 2. (b) Case 3.

inverter outside nominal operations, which are previously studied in [3]. Figure 2(a) is the switch-voltage waveform, which does not reach zero prior to the turn-on instant. This switching pattern is called as "Case 1". Conversely, when the switch voltage reaches zero prior to the turn-on instant, the MOSFET antiparallel body diode turns ON, as shown in Fig. 2(b); this is "Case 2". In Case 2, ZVS is achieved at $\theta = \theta_1$ because of the MOSFET body diode. During the MOSFET body diode is in ON state, the switch current is negative. There is a case that the switch voltage returns to positive at $\theta = \theta_2$ via MOSFET-body-diode ON state, as shown in Fig. 2(c), which is "Case 3". This switching pattern occurs when the switch current becomes positive during the anti-parallel diode is in ON state.

2.2. Class-E Rectifier

The class-E rectifier consists of diode D as a switching device, shunt capacitance C_D, low-pass filter network $L_f - C_f$, and load resistance R. The waveforms of the class-E rectifier is reversed version of those of the class-E inverter, as shown in Fig. 1(b). The diode works as a half-wave voltage rectifier and the rectified voltage is converted into dc voltage through the low-pass filter $L_f - C_f$. At the turn-off transition of the diode, both the diode voltage v_D and the slope of it $dv_D/d\theta$ are zero as shown in Fig. 1(b), which are also the class-E ZVS/ZDS conditions. Therefore, the class-E rectifier can also achieve the high power conversion efficiencies at high frequencies.

Unlike the class-E inverter, the class-E rectifier has only one switching pattern, as shown in Fig. 1(b). This is because the diode in the rectifier can autonomously achieve the class-E ZVS/ZDS conditions regardless of circuit-parameter variations.

3. Waveform Equations Outside Nominal Operations

In this section, the analysis of the class-E^2 dc-dc converter is carried out. The analytical expressions in the previous studies [1], [3] are the basis for the analysis in this paper.

3.1. Assumptions

The analysis in this paper is based on the following assumptions for simplification.

a) The MOSFET works as an ideal switch device. In particular, it has zero on-resistance, infinite off-resistance and zero switching time.

b) The MOSFET body diode and the diode in the rectifier also work as ideal switch devices. Therefore, it has zero forward voltage drop, infinite off-resistance, and zero switching time.

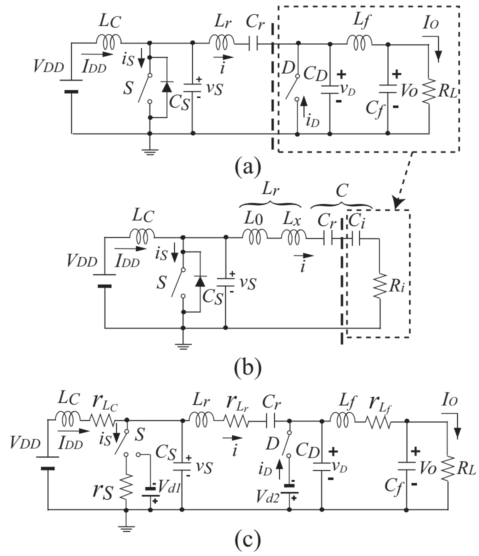

Figure 3: Equivalent models of class-E^2 dc-dc converter. (a) Model for deriving waveform equation. (b) Typical class-E inverter model. (c) Loss calculation model.

c) The dc-feed inductance L_C is high enough so that the current through the dc-feed inductor is constant.

d) The loaded Q-factor is high enough to generate a pure sinusoidal output current i for any parameters.

e) All the passive elements are linear and have zero equivalent series resistance (ESR).

f) The circuit operations are considered in the interval $0 \le \theta < 2\pi$. The switch is in the off-state for $0 \le \theta < 2\pi D_1$ and in the on-state for $2\pi D_1 \le \theta < 2\pi$.

g) The MOSFET body diode turns on at $\theta = \theta_1$ and turns off at $\theta = \theta_2$ for $0 < \theta_1 \le \theta_2 < 2\pi D_1$. When θ_1 and/or θ_2 does not appear during switch-off interval, this analysis gives $\theta_1 = 2\pi D_1$ and/or $\theta_2 = 2\pi D_1$, respectively.

From the above assumption, the equivalent circuit of the class-E^2 dc-dc converter is obtained, as shown in Fig. 3(a).

3.2. Class-E Rectifier

The input current of the rectifier i, which flows through the $L_r - C_r$, is

$$i = \sqrt{2} I_m \sin(\theta + \phi_1) \tag{2}$$

where I_m and ϕ_1 are the effective value of i and the phase shift between the driving signal of the inverter and input current of the rectifier, as shown in Fig. 1(b). From [1], output current I_o is

$$I_o = \frac{V_o}{R_L} = \sqrt{2} I_m \sin\phi_d, \tag{3}$$

where V_o, R_L, and ϕ_d are output voltage, load resistance , and phase shift between i and the diode voltage v_D, respectively. ϕ_d can be obtained from

$$\tan\phi_d = \frac{1 - \cos(2\pi D_d)}{2\pi(1 - D_d) + \sin(2\pi D_d)}. \tag{4}$$

where D_d is the diode-on duty ratio. The relationship among D_d and the rectifier components is expressed as

$$\omega C_D R_L = \frac{1}{2\pi}\left\{1-\cos(2\pi D_d)-2\pi^2(1-D_d)^2 + \frac{[2\pi(1-D_d)+\sin(2\pi D_d)]^2}{1-\cos(2\pi D_d)}\right\}. \quad (5)$$

The diode current i_D is

$$i_D = \begin{cases} I_o - i, & \text{for diode on state} \\ 0, & \text{for diode off state,} \end{cases} \quad (6)$$

The class-E rectifier can be replaced by the equivalent input capacitance C_i and the equivalent input resistance R_i, which are connected in serial, as shown in Fig. 3(b). From [1], the equivalent input capacitance C_i and the equivalent input resistance R_i are

$$C_i = \pi C_D\Big[\pi(1-D_d)+\sin(2\pi D_d)-\frac{1}{4}\sin(4\pi D_d)\cos(2\phi_d) -\frac{1}{2}\sin(2\phi_d)\sin^2(2\pi D_d)-2\pi(1-D_d)\sin\phi_d\sin(2\pi D_d-\phi_d)\Big]^{-1}, \quad (7)$$

and

$$R_i = 2\cdot R_L\cdot\sin^2\phi_d. \quad (8)$$

The class-E^2 dc-dc converter is transformed into the typical class-E inverter because of these equivalent components, as shown in Fig. 3(b). Therefore, the analytical expressions of the class-E inverter outside nominal conditions in previous study [3] can be applied to the class-E^2 dc-dc converter.

3.3. Class-E Inverter

From [3], the switch voltage is given by

$$v_S = \begin{cases} \dfrac{1}{\omega C_S}\{I_{DD}\theta + I_m[\cos(\theta+\phi_1)-\cos\phi_1]\}, & \text{for } 0\le\theta<\theta_1 \\ 0, & \text{for } \theta_1\le\theta<\theta_2 \\ \dfrac{1}{\omega C_S}\{I_{DD}(\theta-\theta_2) + I_m[\cos(\theta+\phi_1)-\cos(\theta_2+\phi_1)]\}, & \text{for } \theta_2\le\theta<2\pi D_1 \\ 0, & \text{for } 2\pi D_1\le\theta<2\pi \end{cases} \quad (9)$$

where I_{DD} is the dc-supply current.

Because of assumption c), the dc voltage drop across the choke inductor L_C is zero. Therefore, the dc-supply voltage is

$$V_{DD} = \frac{1}{2\pi D_1}\int_0^{2\pi D} v_S\, d\theta. \quad (10)$$

In this analysis, L_r is divided into L_0 and L_x, where L_0 and C are ideal resonant filter for ω and C is the composite capacitances of C_r and C_i, as shown in Fig. 3(b). By applying Fourier analyses, the voltage amplitudes on R_i and L_x are

$$R_i I_m = \frac{1}{\pi D_1}\int_0^{2\pi D_1} v_S\sin(\theta+\phi_1)d\theta, \quad (11)$$

and

$$L_x I_m = \frac{1}{\pi D_1}\int_0^{2\pi D_1} v_S\cos(\theta+\phi_1)d\theta. \quad (12)$$

From (10), (11), and (12), I_m, ϕ_1, and I_{DD} can be derived analytically.

The current through the switch and body diode i_S is

$$i_S = \begin{cases} 0, & \text{for } 0\le\theta<\theta_1 \\ I_{DD}-I_m\sin(\theta+\phi_1), & \text{for } \theta_1\le\theta<\theta_2 \\ 0, & \text{for } \theta_2\le\theta<2\pi D_1 \\ I_{DD}-I_m\sin(\theta+\phi_1), & \text{for } 2\pi D_1\le\theta<2\pi, \end{cases} \quad (13)$$

θ_1 and θ_2 can be obtained from the algorithm previously reported in [3].

4. Output Power and Power Conversion Efficiency

Analytical expressions for the output power and the power-conversion efficiency are derived by using the waveform equations given in Section 3. In real circuits, the power losses occur in ESRs of passive elements, MOSFET on-resistance, MOSFET body diode, and diode in the rectifier. Additionally, the switching loss of the MOSFET occurs in Case 1 and Case 3. Figure 3(c) shows the equivalent circuit model of the class-E^2 dc-dc converter for the power-loss calculations. In this paper, the power losses in MOSFET on-resistance r_S; ESRs of dc-feed inductance r_{L_C}, resonant network r_{L_r}, and low pass filter inductance r_{L_f}; turn-on switching loss; and forward voltage drops of MOSFET-body-diode V_{d1}, and diode in the rectifier V_{d2} are considered. Because the ESRs of capacitances are significantly small compared with those of inductances, the power losses in the capacitances are ignored in this paper. It is assumed that the parasitic resistances and MOSFET-body-diode forward voltage drop are small enough not to affect the waveforms as stated in the analysis [3]. The analytical expressions of the power losses can be derived by following the analysis [3]. These are omitted in this paper due to space limitations.

The output power P_o is

$$P_o = R_L I_o^2. \quad (14)$$

The power conversion efficiency is obtained as

$$\eta = \frac{P_o}{P_o+P_S+P_{L_C}+P_{L_r}+P_{L_f}+P_{SW}+P_{D_S}+P_D}, \quad (15)$$

where P_S, P_{L_C}, P_{L_0}, P_{L_f}, P_{SW}, P_{D_S}, and P_D are conduction losses of r_S, r_{L_C}, r_{L_r}, and r_{L_f}, turn-on switching loss, and conduction losses of the MOSFET body diode and the diode in the rectifier, respectively.

5. Experimental Verification

For validating the analytical expressions, circuit experiments were carried out. The design specifications for nominal operation were given as follows: operating frequency f = 1 MHz, dc-supply voltage V_{DD} = 12 V, output power P_o = 5 W, output resistance R_{Lnom} = 50 Ω, switch-off duty ratio D_1 = 0.5, and loaded quality factor $Q = \omega L_0/R_i$ = 10, where the subscription "nom" means the parameter value under nominal conditions. First, we carry out the design of the class-E inverter with the nominal conditions in (1). By using design equations in [5], the design values were obtained. The low-pass network L_f –

Table 1: Analytical results and experimental measurements for nominal condition

	Analytical	Measured	Difference
V_{DD}	12.0 V	12.0 V	0.00 %
D_1	0.5	0.5	0.00 %
f_{nom}	1 MHz	1 MHz	0.00 %
R_{Lnom}	50.0 Ω	49.5 Ω	1.00 %
D_d	0.416	-	-
L_C	115 μH	120 μH	4.5 %
L_r	26.4 μH	26.5 μH	0.26 %
L_f	300 μH	324 μH	8.0 %
C_S	1.76 nF	1.75 nF	−0.58 %
C_r	1.32 nF	1.32 nF	−0.20 %
C_D	2.27 nF	2.22 nF	−2.1 %
C_f	470 μF	-	-
r_S	-	0.16 Ω	-
r_{L_C}	-	0.018 Ω	-
r_{L_r}	-	0.48 Ω	-
r_{L_f}	-	0.025 Ω	-
V_{d1}	-	0.7 V	-
V_{d2}	-	0.75 V	-
P_o	5.0 W	4.82 W	−3.6 %
η	91.7 %	91.1 %	−0.67 %

C_f were selected to be 300 μH and 470 μF, which are sufficiently large for generating the dc-output voltage with low ripple. An IRF530 MOSFET and STTH302 diode were used in the circuit experiment. Therefore, r_S = 0.16 Ω, $V_{d1} = 0.7$ V, and $V_{d2} = 0.75$ V were obtained from IRF530 and STTH302 datasheets. All element values including ESR values were measured by a HP4284A LCR impedance meter. In experimental circuits, the shunt capacitance was composed of the MOSFET drain-to-source capacitance and external one connected in parallel. The IRF530 MOSFET drain-to-source capacitance was estimated as 480 pF, which is obtained from the datasheet. The analytical predictions and experimental measurements for satisfying the class-E ZVS/ZDS conditions were given in Table 1. Figure 4 shows the analytical and experimental waveforms of the nominal operation. It is seen from Fig. 4 that both analytical and experimental waveforms achieved the class-E ZVS/ZDS conditions in this state.

5.1. Output Power and Power Conversion Efficiency

The output power and the power conversion efficiency as a function of R_L/R_{Lnom} were shown in Fig. 5. It is seen from Figs. 5 that the analytical predictions quantitatively agreed with the the experimental measurements, which validated the accuracy and effectiveness of the analytical expressions in this paper. There is the Case 2 region, particularly ZVS region, for $R_L/R_{Lnom} \le 1$, as shown in Fig. 5. Although it is known that ZVS can be achieved for $0 \le R_L \le R_{Lnom}$ on the class-E^2 dc-dc converter [1], there is no paper that shows the region analytically. By using the analytical expressions presented in this paper, the region can be obtained analytically.

6. CONCLUSION

In this paper, steady-state analysis of the class-E^2 dc-dc converter outside nominal conditions has been presented. Steady-state behaviors of the class-E^2 dc-dc converter outside nominal conditions can be investigated by using the analytical expressions derived in this paper. By carrying out the circuit experiments, it is shown that the analytical predictions agreed with the experimental results quantitatively, which validates the accuracy of our analytical expressions.

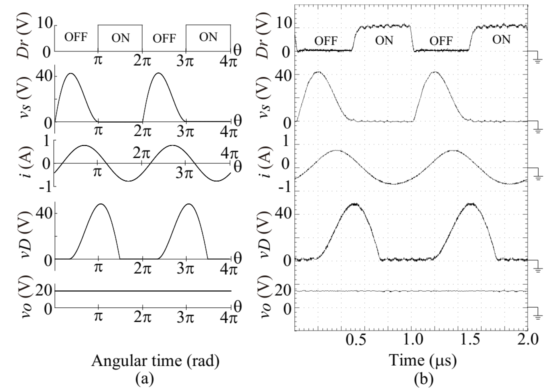

Figure 4: Waveforms of nominal operation. (a) Analytical waveforms. (b) Experimental waveforms.

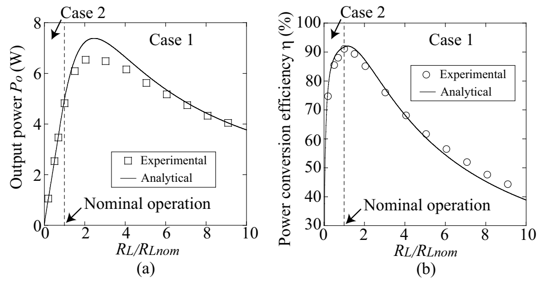

Figure 5: Output power and power conversion efficiency as a function of R_L/R_{Lnom}. (a) Output power. (b) Power conversion efficiency.

References

[1] M. K. Kazimierczuk and J. Jozwik, "Resonant DC/DC converter with class-E inverter and class-E rectifier," *IEEE Trans. Ind. Electron.,* vol.36, no.4, pp. 468–478, Nov. 1989.

[2] J. Jozwik and M. K. Kazimierczuk, "Analysis and design of class-E^2 DC/DC converter," *IEEE Trans. Ind. Electron.,* vol. 37, no. 2, pp. 173–183, Apr. 1990.

[3] T. Nagashima, X. Wei, T. Suetsugu, M. K. Kazimierczuk, and H. Sekiya, "Waveform equations, output power, and power conversion efficiency for class-E inverter outside nominal operation," *IEEE Trans. on Ind. Electron.,* vol. 61, no. 4, pp. 1799–1810, Apr. 2014.

[4] M. K. Kazimierczuk, "Analysis of class E zero-voltage switching rectifier," *IEEE Trans. Circuit Syst.,* vol. 37, no. 6, pp. 747–755, Jun. 1990.

[5] M. K. Kazimierczuk and D. Czarkowski, *Resonant Power Converters 2nd Ed*, New York, NY: John Wiley & Sons, 2011.